Bull. Ind. Soc. Earth. Tech., Paper No.368, Vol.34 No.3, Sept. 1997, pp 137- 158

AN INTEGRATED PGA ATTENUATION RELATIONSHIP

By I.D. Gupta[1], V. Rambabu[2] and B.M. Rame Gowda[3]
Central Water & Power Research Station, Khadakwasla, Pune–411024, India

ABSTRACT

Using several well behaved empirical attenuation relations for peak ground acceleration (PGA), developed by various investigators for different parts of the world, an integrated relationship has been developed to normalize for the effects of regional variations in the attenuation characteristics. Simple source–mechanism considerations have been applied to suitably modify the integrated PGA attenuation relationship to get realistic estimates of the peak acceleration values at near–field distances. For a case where site specific relation is not available, the presented relationship would provide more stable and least biased value of peak acceleration compared to that obtained from an arbitrarily chosen relationship for another region.

INTRODUCTION

The drawbacks and difficulties associated with the use of standard spectral shapes (Seed et al., 1976; Mohraz, 1976; Housner, 1959) normalized by peak ground acceleration (PGA) are now well recognized (Trifunac, 1992). To overcome these difficulties, several improved procedures have been suggested by different investigators to arrive at more reliable site specific design earthquake ground motion (Anderson and Trifunac, 1978; Gupta, 1991; Gupta and Joshi, 1996ab; Lee, 1989; 1993; Trifunac, 1978; etc.). However, the use of a standard spectrum and the peak ground acceleration is likely to remain popular for quite some time, due to its simplicity and familiarity among practising engineers. In this approach, in addition to the difficulties in selecting a suitable shape of the spectrum in an unambiguous way, it is also very difficult to obtain an accurate and reliable estimate of the PGA for specified parameters of a design earthquake (magnitude and source–to–site distance).

The peak ground acceleration is a highly unstable parameter (Gupta, 1994) and its correlation with earthquake magnitude and distance is characterized by large scattering and uncertainties. The earthquake magnitude is conventionally defined from the peak amplitude of intermediate or long–period seismic waves (Richter,1958), whereas the peak acceleration is mostly associated with the high frequency waves. In the near field, very close to the seismic source, the peak acceleration is mainly governed by the stress drop (Brune, 1970) and not by the magnitude. Due to the use of different data bases, various published empirical attenuation relations for peak ground acceleration produce

1. Chief Research Officer
2. Assistant Research Officer
3. Joint Director

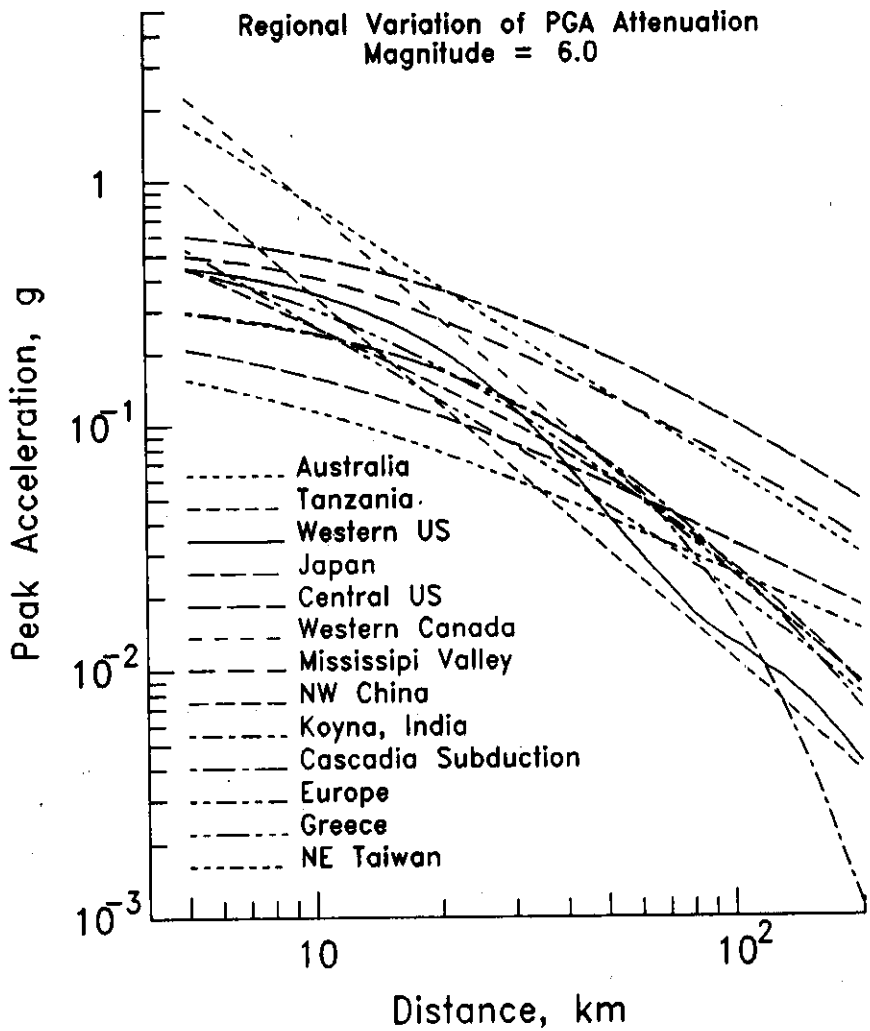

Fig.1 A typical plot for M = 6.0 of several attenuation relations developed by various investigators for different parts of the world.

widely varying results. Thus it becomes difficult to select a relationship which can be considered appropriate for a specific application. Further, the use of a particular relationship for an area with different geological and tectonic features would lead to the results which may differ significantly from the actual values.

To get consistently stable estimates of the PGA values with minimal deviations from the real values for a wide range of earthquake parameters, several well behaved published attenuation relations have been integrated together to develop an average attenuation relationship in the present study. This relationship has been then modified for the near–source saturation effects to get realistic values of PGA at very small source–to–site distances. For the cases where site specific data are lacking, the use of the proposed integrated relationship would be better than arbitrarily using a specific relationship for another region.

ANALYSIS OF AVAILABLE RELATIONSHIPS

A large number of PGA attenuation relations have been developed by various investigators using different sets of recorded data from several parts of the world. Paul et al. (1978) and Campbell (1985) have reviewed the attenuation relationships published upto around 1984. A set of 35 published relations, which include several recent and many popularly used past relationships, has been considered for the present study. These relations are listed in Appendix–A. A typical plot of the attenuation relations for several different regions, evaluated with magnitude 6.0, is given in Fig. 1. From this figure it is seen that there may be large regional variations in the attenuation characteristics, and the use of an attenuation relation from some other region may not be suitable. To minimize such errors, the regional differences have been averaged out by developing an integrated attenuation relationship using all the well behaved relationships from Appendix–A.

To scrutinize the behavior of the attenuation relations given in Appendix–A, the peak acceleration values computed for M = 4.0, 5.0, 6.0, 7.0 and 8.0 were plotted as a function of distance for each of the relationships. Some typical examples of the attenuation relations depicting abnormal behavior are plotted in Fig. 2. The relationship # 01 is seen to increase linearly to very large values at small distances and it attenuates at very slow rate for distances beyond 70 km. The relationship # 02 as shown in Fig. 2, and also # 06 to # 08, # 11 to # 13, # 18 and # 23 are all found to increase linearly to very large values with decrease in distance. These relations grossly overestimate the near–field acceleration values and are thus not suitable. On the other hand, relationship # 04 underestimates the peak acceleration for small magnitudes at large distances and vice–versa. Relation # 16 for rock sites shows very slow attenuation with distance and unrealistically small variation with magnitude, whereas relation # 21 for central US is seen to have unrealistically slow decay with distance and fast increase with magnitude. Several relations (for example, # 20 as shown in Fig. 2 and # 03 and # 27 for NE China) underestimate the PGA for small magnitudes and grossly overestimate that for

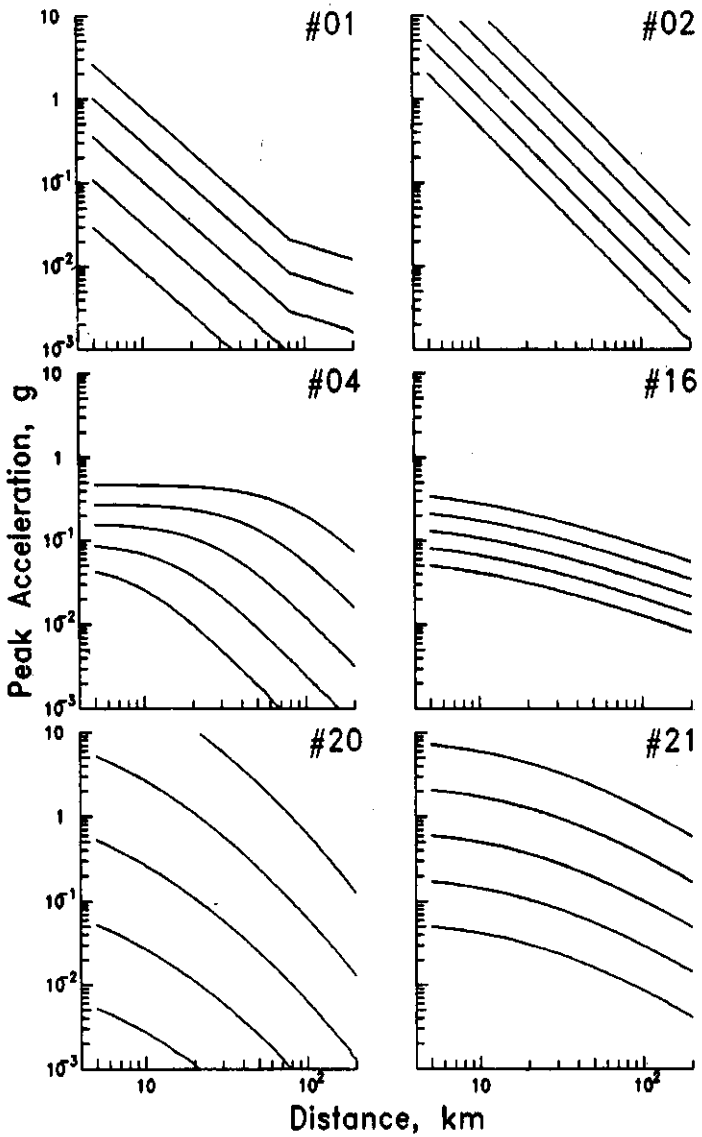

Fig.2 Plot for M = 4.0, 5.0, 6.0, 7.0 and 8.0 of some typical attenuation relations which show abnormal behaviour and hence not used in developing the present integrated relationship. The numbers for various plots correspond to the serial numbers given to various attenuation relations in Appendix-A.

large magnitudes. Thus, after deleting all the above mentioned attenuation relations, only 22 well behaved remaining relations have been used for further study.

INTEGRATED ATTENUATION RELATIONSHIP

The mean value, μ, and the standard deviation, σ, of the PGA values obtained from the 22 well behaved relationships were computed for nine magnitude values equal to 4.0, 4.5, 5.0, ..., 8.0, and 196 distances from 5 km to 200 km at an interval of 1.0 km. By plotting these relationships along with the $(\mu \pm \sigma)$ band for each of the nine magnitudes, it was observed that some of the relations lie far outside the $(\mu \pm \sigma)$ band or deviate significantly from the mean trend of attenuation for certain magnitude and distance ranges. Dashed curves in Figs. 3(a) and 3(b) show typical examples of such relations or parts of relations which have been discarded from further analysis. The least squares regression analysis of the peak acceleration values for the above mentioned nine magnitudes and 196 distances as obtained from the 22 selected empirical attenuation relations, only for the magnitude and distance ranges over which each relation shows consistent behavior with the $(\mu \pm \sigma)$ band, leads to the following integrated attenuation relationship

$$\ln a = -5.7864 - 0.7023 \ln R - 0.005577R + 1.2164M - 0.0372M^2; \quad \sigma_{\ln a} = 0.3546 \tag{1}$$

In this equation, a is the peak acceleration in units of acceleration due to gravity (g), M is the earthquake magnitude and R is a measure of the source–to–site distance. The mathematical form of eqn. (1) is based on the physical principles of seismology and elastic wave–propagation (Gupta, 1994). For example, first term is related to the strength of earthquake source, second term accounts for geometrical spreading of wave energy, the third term describes the anelastic attenuation and the fourth and fifth terms give the magnitude scaling, where quadratic dependence has been selected to achieve the magnitude saturation effects.

The relationship of eqn. (1) is found to describe very well the attenuation of PGA for intermediate and large distances, but the peak acceleration is seen to blow up for very small distances. This is because this relationship is not able to consider the effect of near distance saturation of the peak acceleration (Gupta et al., 1994). Most of the published attenuation relations used to develop the relationship of eqn. (1) are based on strong motion data recorded at distances greater than about 20 km. Thus, the extrapolation of eqn. (1) to very small distances gives unrealistically high values of peak acceleration, particularly for large magnitudes. To compute the peak acceleration in the near field, eqn. (1) is required to be modified to consider the saturation effects.

MODIFICATION FOR SATURATION EFFECTS

Almost all the available empirical attenuation relations are based on the point source approximation, according to which the entire seismic energy is assumed to originate from a point, and the source–to–site distance, R, refers to that point only. This

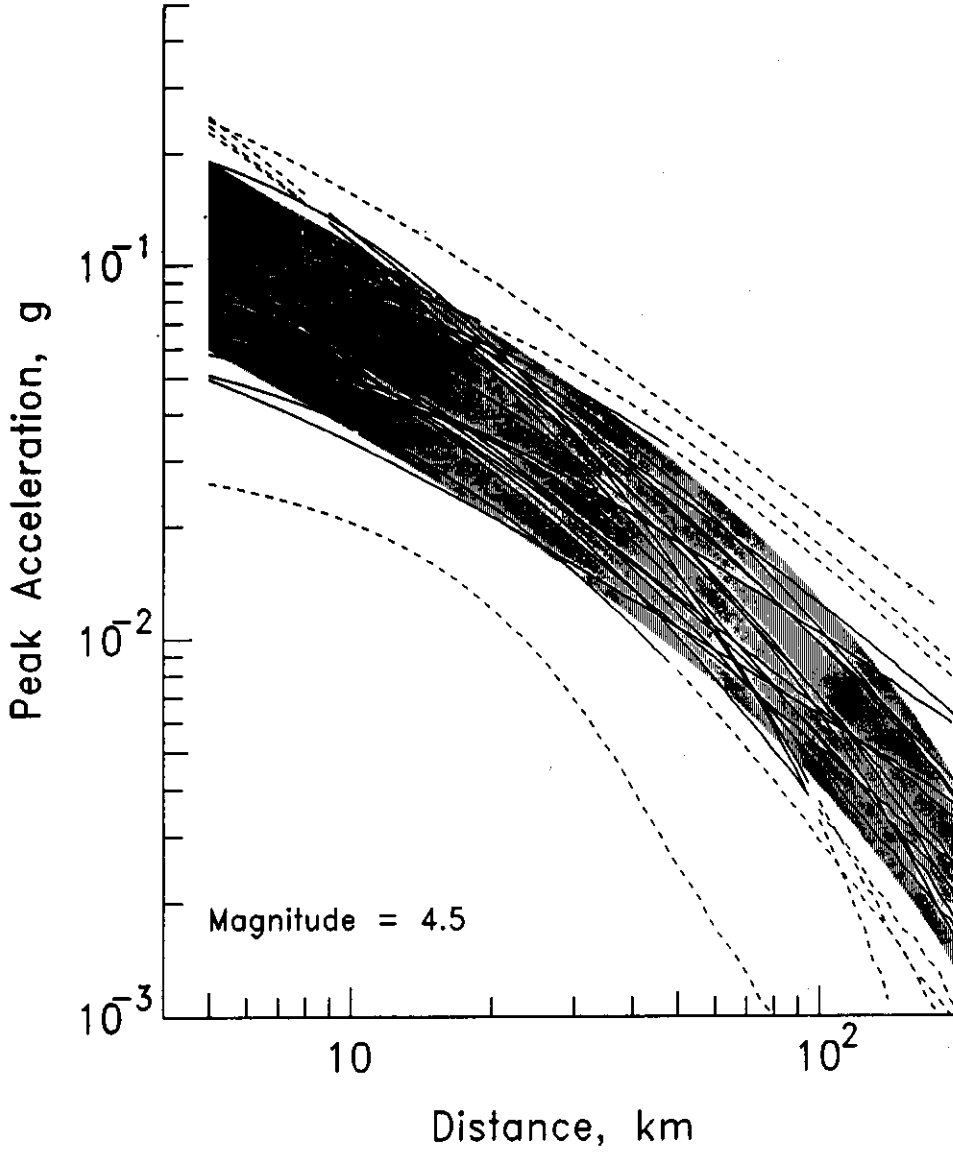

Fig.3(a) Comparison of 22 well behaved attenuation relations (various curves) for M=4.5 with their ($\mu \pm \sigma$) band (grey zone). The curves or parts of curves plotted by dashed lines have not been considered for developing the integrated relationship in the present study.

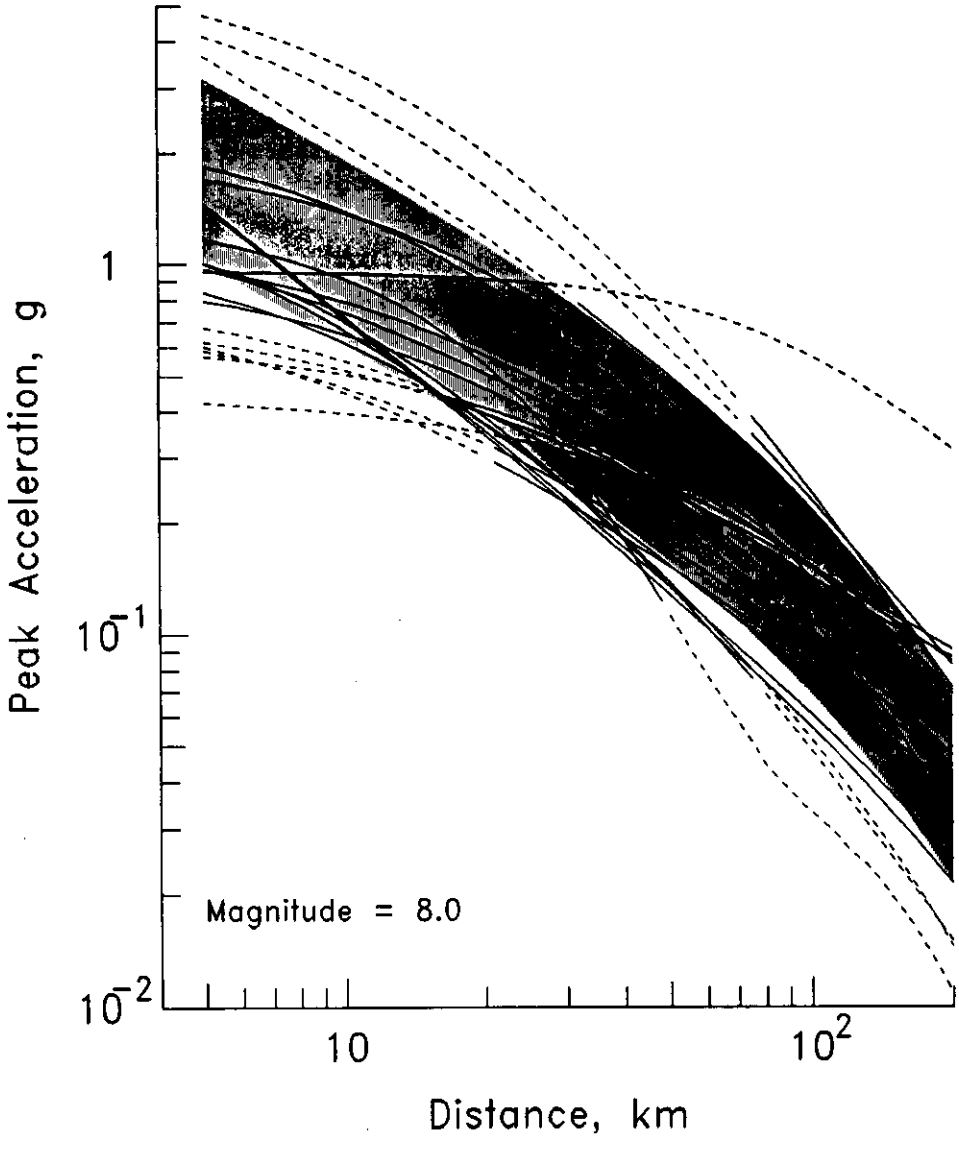

Fig.3(b) Comparison of 22 well behaved attenuation relations (various curves) for M=8.0 with their ($\mu \pm \sigma$) band (grey zone). The curves or parts of curves plotted by dashed lines have not been considered for developing the integrated relationship in the present study.

assumption doesn't make much difference at large distances, but as one approaches closer to the source, the finite size of the fault starts exhibiting its effect. Close to a fault, the point of observation is influenced only by the energy radiated from a limited portion of the fault, and not by the entire fault (Gupta et al., 1994). By idealizing the fault plane by a circular area of radius R_o and assuming the site of observation to lie at a distance R on the axis of the circle, the effect of the finite size of the fault can be accounted in an approximate but very simple way by replacing the distance R with an equivalent distance R_{eq}, defined as (Appendix-B)

$$R_{eq} = R_o \left[\ln \left(\frac{R^2 + R_o^2}{R^2} \right) \right]^{-1/2} \tag{2}$$

The various available relationships correlating size of a fault with the earthquake magnitude refer to the total rupture length and are normally associated with very large uncertainties (Wells and Coppersmith, 1994). Because the peak ground acceleration in the near field is not governed by the total area of the fault, such relations are not suitable to define the radius R_o for computing the equivalent source-to-site distance. Further, as explained in Gupta et al. (1994), during a large magnitude earthquake involving a large fault rupture area, due to inhomogeneous distribution of tectonic stresses, non-uniform strength of the rock and randomly distributed asperities along a fault plane, the fault ruptures in a random way in several small patches with different stress drops and dislocations. The strong earthquake ground motion in the near-field is governed only by a limited number of such patches closest to the site. Thus to get a realistic estimate of the equivalent distance from eqn. (2), it is necessary to use the effective size of the fault, rather than its actual physical size. Though there is no way to find the actual effective size of a fault generating an earthquake, the empirical relations due to Trifunac and Lee (1990) can be used to conveniently obtain it for practical applications.

By performing regression analysis of the Fourier spectrum amplitudes of a large number of strong-motion records, Trifunac and Lee (1990) have developed scaling relations for the effective source size as a function of the wave-period and earthquake magnitude. Because the peak ground acceleration is normally associated with the high-frequency waves, in the present study, the effective radius R_o of the fault has been taken equal to half the source size S for the lowest period range (0.04 - 0.10 sec) defined by Trifunac and Lee as

$$S = 0.2 + 8.23(M - 3); \quad R_o = S/2 \tag{3}$$

The equivalent distance R_{eq} evaluated using this R_o would be able to account for the near-distance saturation effects in a very simple way. Fig. 4 shows the comparison of the peak acceleration values (dashed curves) obtained directly from the attenuation relationship of eqn. (1) with those (solid curves) obtained by substituting R_{eq} in place of R in eqn. (1). It is apparent that the use of the equivalent distance based on the effective source-size is able to introduce the near-source saturation effects in a quite realistic way. However, to avoid the explicit computation of equivalent distance for use

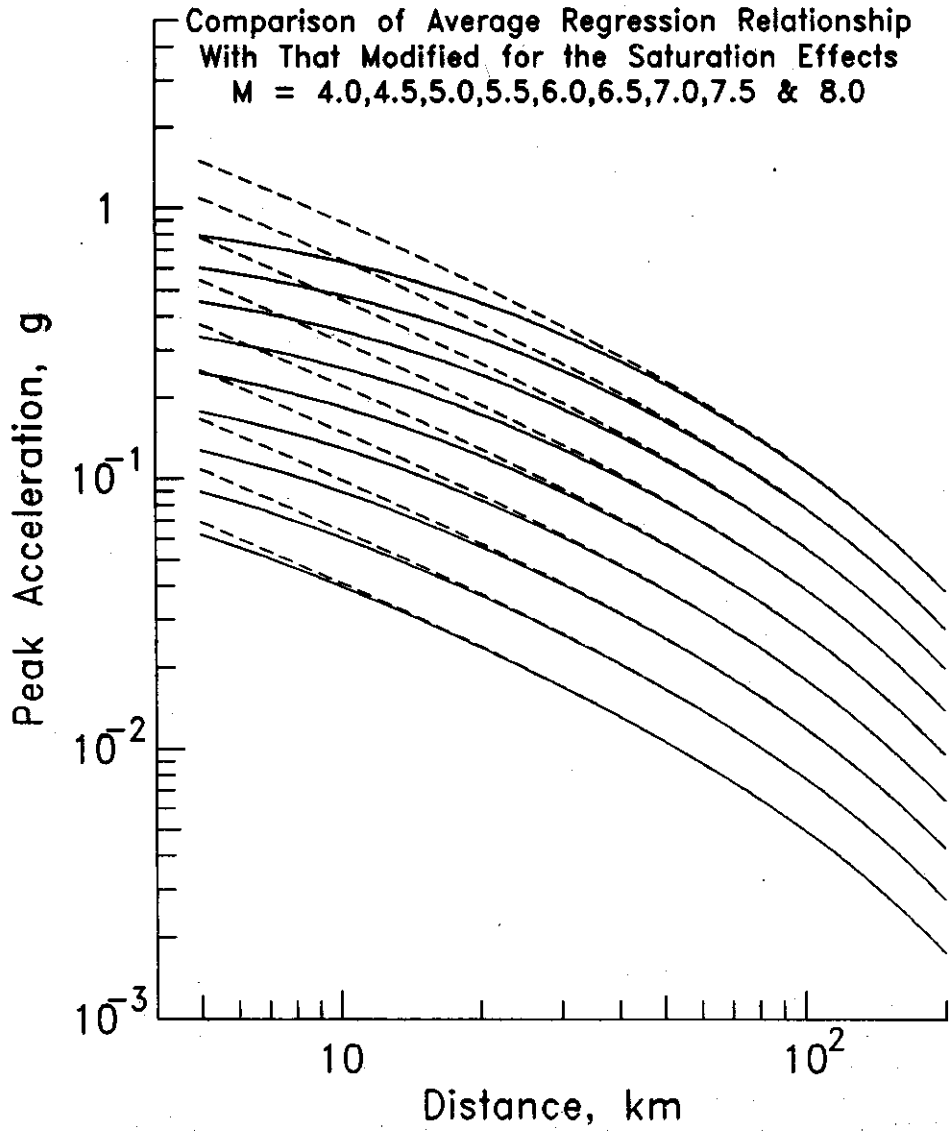

Fig.4 Comparison of the peak acceleration values (dashed curves) obtained from the mean attenuation relationship of eqn. (1) with the corresponding values (solid curves) estimated by considering the near-distance saturation effects. For large magnitudes and very small distances, the solid curves are seen to provide more realistic peak acceleration values.

in the relationship of eqn. (1), the data corresponding to the solid curves in Fig. 4 have been used to obtain the following regression relationship

$$\ln a = -5.3659 + 1.1886M - 0.7842\ln(R + 1.0e^{0.302M}) - 0.005235R - 0.03357M^2; \quad \sigma_{\ln a} = 0.3546 \tag{4}$$

The relationship of eqn. (4), plotted by dashed curves in Fig. 5, is seen to approximate very closely the solid curves of Fig. 4, which are also plotted in Fig. 5 for comparison. Thus the attenuation relationship of eqn. (4) is able to account for the near-distance saturation effects and it also gives the results which are inherently the average of the PGA values obtained from the 22 selected relationships. This equation can, therefore, be considered independent of regional influences and biases.

DISCUSSION AND CONCLUSIONS

Various PGA attenuation relationships, developed by regression analysis of recorded data, are found to be associated with large scattering of the observed data about the mean trends. Thus, even a site specific attenuation relationship is able to provide only the expected value of peak acceleration for engineering applications, and not the true acceleration which may occur during a future design earthquake. Further, the attenuation relations based on the data from different parts of the world are seen to have large regional variations (Fig. 1). Hence, it becomes very difficult to choose a suitable relationship for a region lacking in recorded strong-motion data. In fact, the PGA values obtained from a specific relationship may in some cases be highly biased and in large errors. Therefore, a better approach for engineering applications is to evaluate the mean acceleration value from several attenuation relationships. To facilitate this task, in this paper, an average relationship has been developed by integrating together 22 well behaved published PGA attenuation relations.

The source-to-site distance, R, in all the available attenuation relations refer to a fixed point on the fault, which has been selected by different investigators in several different ways. Some commonly used measurements of R are the epicentral distance, hypocentral distance, closest distance to rupture-area of the fault or its projection on the earth's surface, closest distance to the zone of energy release and the distance to the center of energy release, etc.. But assuming the entire seismic energy to be concentrated at a point is not realistic. The PGA values obtained from the attenuation relations based on the point source approximation are seen to blow-up for distances less than about 20 km, where the finite size of the fault starts exhibiting its effect. Therefore, to get accurate estimates of PGA at very close distances to the fault, in the present study, an approximate empirical procedure has been proposed to modify the integrated relationship (developed from 22 selected attenuation relations) for the near-distance saturation effects. For a region lacking in the recorded data, the present relationship would provide a basis to obtain quite reliable estimates of the peak ground acceleration. Being the average of several well behaved relationships, the results from the proposed

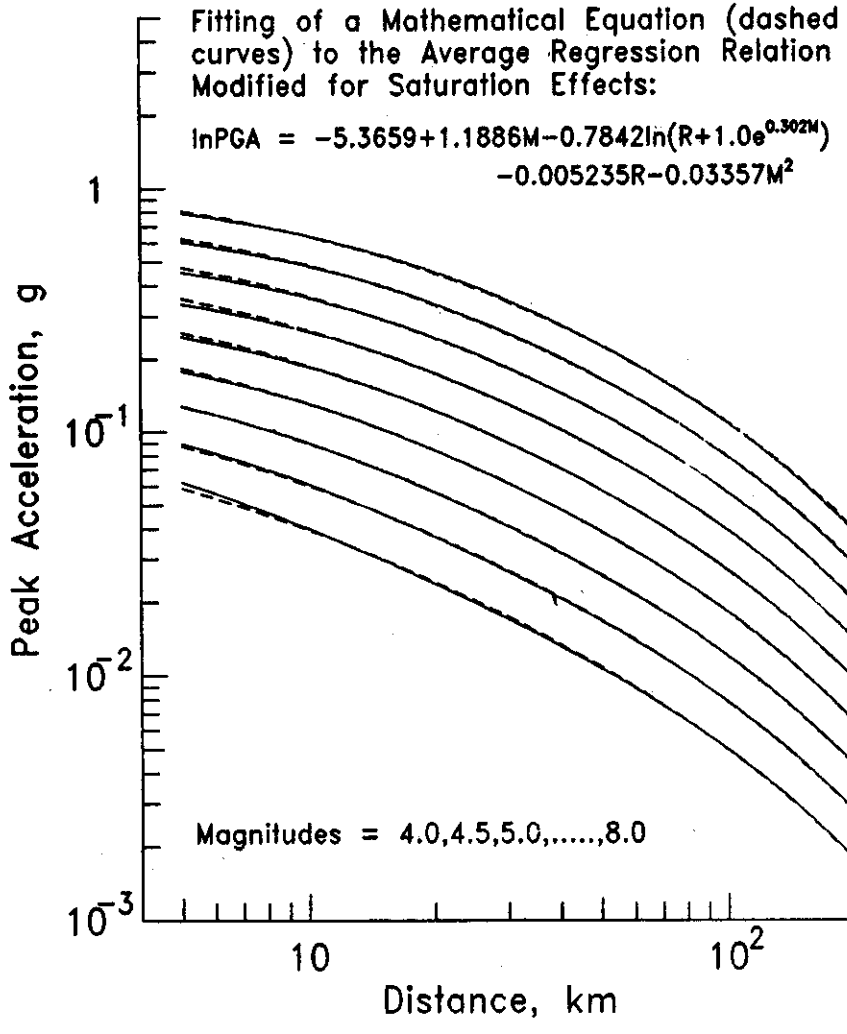

Fig.5 Fitting of a mathematical relationship (dashed curves) to the peak acceleration values (solid curves) obtained by considering the saturation effects.

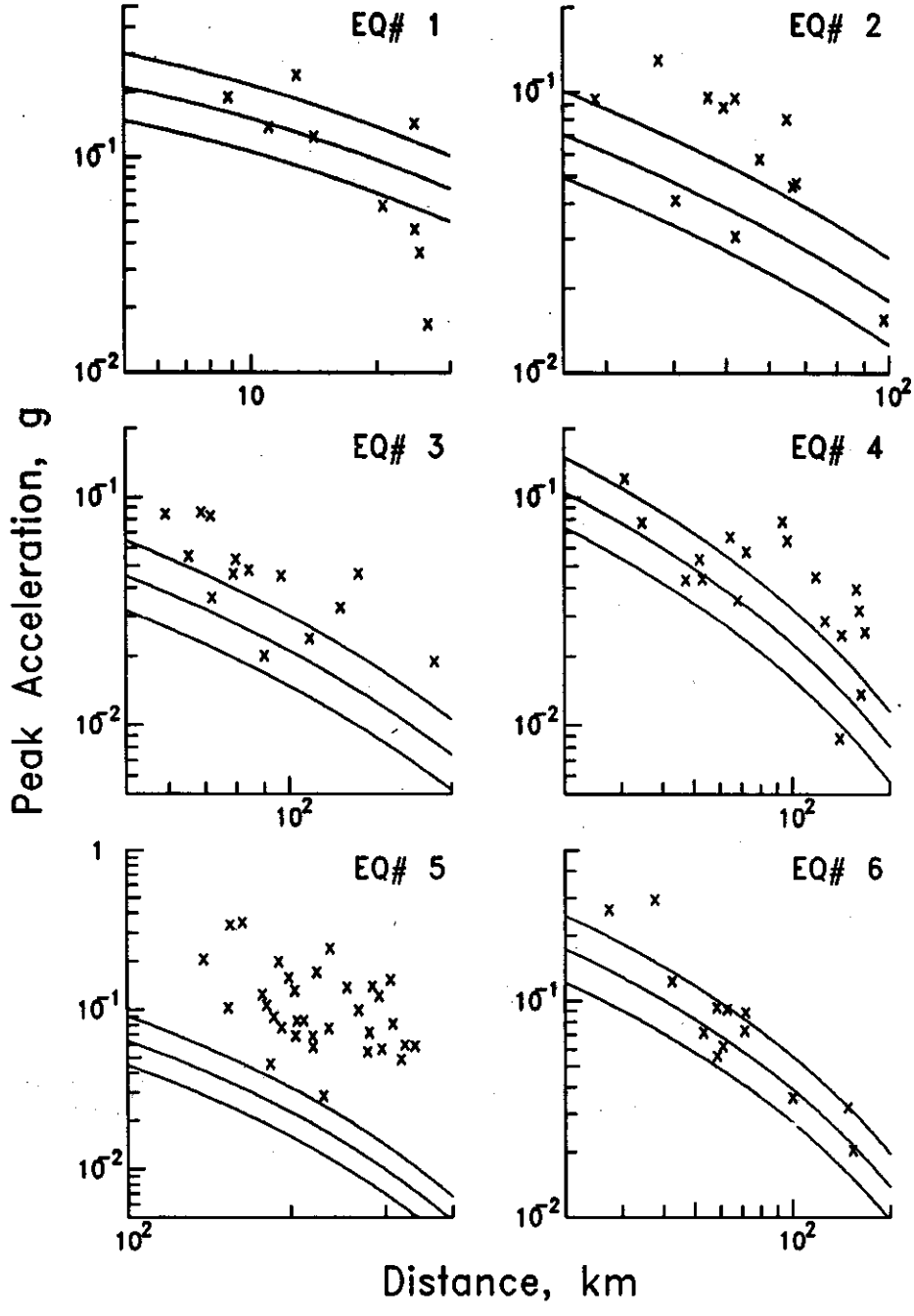

Fig.6 Comparison of the peak acceleration data (discrete symbols) recorded from six earthquakes in the Himalayas with the mean (middle curves) and mean ± one standard deviation (two outer curves) behaviour of the presented integrated attenuation relationship.

relation can be considered more stable than those estimated from a particular relation for another region.

Though the past studies have used several different definitions of the source–to–site distance, a particular measurement of the distance can't be ensured for a future design earthquake. However, due to the finite size of the fault having been taken into account, the way of selecting the source–to–site distance doesn't matter much for the proposed integrated relationship of eqn. (4). Thus, it is recommended to take the distance R in eqn. (4) as the hypocentral distance, which is the most widely used and easily available measurement of the source–to–site distance.

The present integrated relationship corresponds to a single horizontal component of the ground motion. Abrahamson and Litehisher (1989) have made detailed studies on the ratios of vertical to horizontal ground acceleration, which indicates that at close distances this ratio increases from around 0.65 for magnitude 5.0 to about 1.0 for magnitude 8.0. Gupta et al (1991) have found this ratio to be around 0.76 for the strong–motion data recorded in Koyna dam area. Anderson and Lei (1994) have suggested a value of 0.70 for the ratio of vertical to horizontal peak acceleration. Based on these observations it is suggested that the peak vertical acceleration can be taken around 0.70 to 0.75 of the horizontal acceleration obtained from the attenuation relationship of eqn. (4), proposed in the present study.

ACKNOWLEDGEMENT

The authors are very thankful to Dr. B.U.Nayak, Director, CWPRS, Pune for granting his permission to publish this paper.

REFERENCES

1. Abrahamson, N.A. and J.J. Litehiser (1989). Attenuation of vertical peak acceleration, *Bull. Seis. Soc. Am.*, **79**(3), 549–580.

2. Ambraseys, N.M. and J.J. Bommer (1991). The attenuation of ground acceleration in Europe, *Earthq. Engg. and Struc. Dyn.*, **20**, 1179–1202.

3. Anderson, J.G. and M.D. Trifunac (1978). Uniform risk functionals for characterization of strong earthquake ground motion, *Bull. Seis. Soc. Am.*, **68**, 205–218.

4. Anderson, J.G. and Y. Lei (1994). Nonparametric description of peak acceleration as a function of magnitude, distance, and site in Guerrero, Mexico, *Bull. Seis. Soc. Am.*, **84**(4), 1003–1017.

5. Bath, M. (1975). Seismicity of the Tanzania region, *Tectonophysics*, **27**, 353–379.

6. Battis, J. (1981). Regional modification of acceleration functions, *Bull. Seis. Soc. Am.*, **71**, 1309–1321.

7. Brune, J.N. (1970). Tectonic stress and spectra of seismic shear waves from earthquakes, *Jour. Geophys. Res.*, **75**, 4997–5009.

8. Campbell, K.W. (1981). Near-source attenuation of peak horizontal acceleration, *Bull. Seis. Soc. Am.*, **71**, 2039–2070.

9. Campbell, K.W. (1985). Strong motion attenuation relations : A ten-year prospective, *Earthquake Spectra*, **1**(4), 759–804.

10. Cornell, C.A., H. Banon and A.F. Shakal (1979). Seismic motion and response prediction alternatives, *Earthq. Engg. and Struc. Dyn.*, **7**, 295–315.

11. Crouse, C.B. (1991). Ground motion attenuation for earthquakes in the Cascadia subduction zone, *Earthquake Spectra*, **7**(2), 201–236.

12. Davenport, A.G. (1972). A statistical relationship between rock amplitude magnitude and epicentral distance and its application to seismic zoning, Univ. of Western Ontario, Faculty of Engg. Science, BLWT–4–72.

13. Denham, D.G. and G.R. Small (1971). Strong motion data centre, *Bull. New Zealand Soc. of Earthq. Engg.*, **4**, 17.

14. Donovan, N.C. (1973). A statistical evaluation of strong motion data including the Feb. 9, 1971 San Fernando earthquake, *Proc. Fifth World Conf. on Earthq. Engg.*, Rome, **1**, 1252–1261.

15. Donovan, N.C. and A.E. Bornstein (1978). Uncertainties in seismic risk procedures, *Jour. Geotech. Engg. Div., ASCE*, **104**, 869–887.

16. Espinosa, A.F. (1980). Attenuation of strong horizontal ground accelerations in the western United States and their relation to M_L, *Bull. Seis. Soc. Am.*, **70**, 583–616.

17. Esteva, L. (1970). Seismic risk and seismic design decision, in Seismic Design for Nuclear Power Plants, Edt. by R.J. Hansen, MIT Press, Cambridge, 438–483.

18. Esteva, L. and E. Rosenblueth (1963). Espectros de temblores a distancias moderasr grandes, *Proc. Chilean Conf. on Seis. and Earthq. Engg.*, **1**, Univ. of Chile.

19. Esteva, L. and R. Villaverde (1973). Seismic risk design spectra and structural reliability, *Proc. Fifth World Conf. on Earthq. Engg.*, Rome, **1**, 2586–2597.

20. Fukushima, Y. and T. Tanara (1990). A new attenuation relation for peak horizontal acceleration of strong earthquake ground motion in Japan, *Bull. Seis. Soc. Am.*, **80**(4), 757–783.

21. Gupta, I.D. (1991). A note on computing uniform risk spectra from intensity data on earthquake occurrence, *Soil Dyn. and Earthq. Engg.*, **10**, 407–413.

22. Gupta, I.D. (1994). Defining effective peak acceleration via order statistics of acceleration peaks, *European Earthq. Engg.*, **VIII**(2), 3–11.

23. Gupta, I.D. and R.G. Joshi (1996a). Evaluation of Design Earthquake Ground Motion for Soil and Rock Sites, *Workshop on Design Practices in Earthquake Geotechnical Engineering*, Sept.26-27, 1996, Roorkee, India, 58-87.

24. Gupta, I.D. and R.G. Joshi (1996b). An Improved Approach for Evaluation of Site-specific Ground Motion for Earthquake Resistant Design of Dams, *Proc. 2nd International Conf. on Dam Safety Evaluation*, Nov.26-30,1996, Trivandrum, India, 725-736.

25. Gupta, I.D., V. Rambabu and R.G. Joshi (1991). Attenuation of peak acceleration, velocity and displacement at small distances in Koyna dam region, India, *Proc. First Int. Conf. on Seis. and Earthq. Engg.*, 27-29 May,1991, Tehran, Iran, 307-316.

26. Gupta, I.D., T.V.S. Ramakrishna and V.C. Deshpande (1994). Predicting near-source strong ground-motion due to large magnitude earthquakes, *Tenth Symp. on Earthq. Engg.*, I, 16-18.

27. Gutenberg, B. and C.F. Richter (1956). Earthquake magnitude , intensity, energy and acceleration, *Bull. Seis. Soc. Am.*, **46**(2), 105-143.

28. Hasegawa, H.S., P.W. Basham and M.J. Berry (1981). Attenuation relation for strong seismic ground motion, *Bull. Seis. Soc. Am.*, **71**, 2071-2095.

29. Housner, G.W. (1959). Behavior of structures during earthquakes, *Jour. Engg. Mech. Divn., ASCE*, **85**, 109-129.

30 Joyner, W.B. and D.M. Boore (1981). Peak horizontal acceleration and velocity from strong-motion records including records from the 1979 Imperial Valley, California, Earthquake, *Bull. Seis. Soc. Am.*, **71**, 2011-2038.

31. Kanai, K. (1966). Improved empirical formula for the characteristics of strong earthquake motions, *Procs. Japan Earthq. Engg. Symp.*, Tokyo, Japan, 1-4.

32. Lee, V.W. (1989). Empirical scaling of pseudo relative velocity spectra of strong earthquake ground motion in terms of magnitude, and both local soil and geological site classifications, *Earthq. Engg. and Engg. Vibrations*, **9**, 9-29.

33. Lee, V.W. (1993). Scaling PSV from earthquake magnitude, local soil and geological depth of sediments, *Jour. of Geotechnical Engg., ASCE*, **119**, 108-126.

34. Lee, Y.W. (1964). Statistical Theory of Communication, Wiley, New York.

35. McGuire, R.K. (1977). Seismic design spectra and mapping procedures using hazard analysis based directly on oscillator response, *Earthq. Engg. and Struc. Dyn.*, **5**, 211-234.

36. McGuire, R.K. (1978). Seismic ground motion parameter relation, *Jour. Geotech. Engg. Div., ASCE*, **104**, 481-490.

37. Merz H.A. and C.A. Cornell (1973) Seismic risk analysis based on a quadratic magnitude-frequency law, *Bull. Seis. Soc. Am.*, **63**(6), 1999-2006.

38. Mickey, W.V. (1971). Strong motion response spectra, *Earthquake Notes*, **42**, 5-8.

39. Milne, W.G. and A.G. Davenport (1969). Distribution of earthquake risk in Canada, *Bull. Seis. Soc. Am.*, **59**(2), 729-754.

40. Mohraz, B. (1976). A study of earthquake response spectra for different geological conditions, *Bull. Seis. Soc. Am.*, **66**, 915-935.

41. Niazi, M. and Y. Bozorgnia (1991). Behavior of near-source peak horizontal and vertical ground motion over SMART-1 array, Taiwan, *Bull. Seis. Soc. Am.*, **81**(3), 715–732.

42. Nuttli, O.W. and R.B. Herrmann (1984). Ground motion of Mississippi Valley earthquake, *Jour. Tech. Topics in Civil Engg., ASCE*, **110**, 54–69.

43. Orphal, D.L. and J.A. Lahoud (1974). Prediction of peak ground motion from earthquakes, *Bull. Seis. Soc. Am.*, **64**(5), 1563–1574.

44. Paul, D.K., V.N. Singhal and N. Kumar (1978). A guide to acceleration, velocity and displacement relations with distance and magnitude, *Bull. Ind. Soc. of Earthq. Tech.*, **15**(4), 73–88.

45. Peng, K.Z., F.T. Wu and L. Song (1985). Attenuation characteristics of peak horizontal acceleration in Northeast and Northern China, *Earthq. Engg. and Struc. Dyn.*, **13**, 337–350.

46. Richter, C.F. (1958). Elementary Seismology, Freeman, San Francisco.

47. Sabetta, F. and A. Pugliese (1987). Attenuation of peak horizontal acceleration and velocity from Italian Strong-motion records, *Bull. Seis. Soc. Am.*, **77**, 1491–1513.

48. Seed, H.B., C. Ugas and J. Lysmer (1976). Site dependent spectra for earthquake resistant design, *Bull. Seis. Soc. Am.*, **66**, 221–243.

49. Tento, A., L. Franceschina and A. Marcellini (1992). Expected ground motion evaluation for Italian sites, *Proc. Tenth World Conf. on Earthq. Engg.*, 19–24 July 1992, Madrid, Spain, Vol.1, 489–494.

50. Theodulidin, N.P. and B.C. Papazachos (1992). Dependence of strong ground motion on magnitude, distance, site geology and macroseismic intensity for shallow earthquake in Greece, I. peak horizontal acceleration, velocity and displacement, *Soil Dyn. and Earthq. Engg.*, **11**(7), 387–402.

51. Trifunac, M.D. (1976). Preliminary analysis of the peaks of strong earthquake ground motion – dependence of peaks on earthquake magnitude, epicentral distance and recording site condition, *Bull. Seis. Soc. Am.*, **66**(1), 189–219.

52. Trifunac, M.D. (1978). Response spectra of earthquake ground motion, *Jour. of Engg. Mech. Div., ASCE*, **104**, 1081–1097.

53. Trifunac, M.D. (1992). Should peak accelerations be used to scale design spectrum amplitudes ?, *Tenth World Conf. on Earthq. Engg.*, **10**, 5817–5822.

54. Trifunac, M.D. and V.W.Lee (1990). Frequency dependent attenuation of strong earthquake ground motion, *Soil Dyn. and Earthq. Engg.*, **9**(1), 3–15.

55. Wells, D.L. and K.J. Coppersmith (1994). New empirical relationships among magnitude, rupture length, rupture width, rupture area, and surface displacement, *Bull. Seis. Soc. Am.*, **84**, 974–1002.

APPENDIX–A

LIST OF THE PGA ATTENUATION RELATIONS USED IN PRESNT STUDY

1. **Gutenberg, B. and C.F. Richter (1956).**

$$\log a(g) = \log F_a - 2.1 + 0.81M - 0.027M^2$$

$$\log F_a = \begin{cases} -1.029 - 1.725\log R & ; R \leq 75km \\ -3.115 - 0.634\log R & ; R > 75km \end{cases}$$

California region, Rocky ground, focal depth = 15 km

2. **Esteva, L. and E. Rosenblueth (1963).**

$a(cm/s^2) = 2000e^{0.8M}R^{-2}$; Firm ground, Not applicable for $R \leq 15km$

3. **Kanai, K. (1966).**

$$\log a(cm/s^2) = 0.61M - (1.66 + \tfrac{3.6}{R})\log R + (0.167 - \tfrac{1.83}{R}) + 0.6989 - 0.5\log T_G$$

T_G is predominant period of ground.

4. **Milne, W.G. and A.G. Davenport (1969).**

$a(cm/s^2) = \frac{6.77e^{1.64M}}{1.1e^{1.1M}+R^2}$; Applicable to Western region of Canada

5. **Esteva, L. (1970).**

$a(cm/s^2) = 1230e^{0.8M}(R+25)^{-2}$; Firm ground condition

6. **Mickey, W.V.(1971).**

$\log a(cm/s^2) = 1.325 + 0.466M - 1.4\log R$; Not applicable for $R \leq 15$ km

7. **Denham, D.G. and G.R. Small (1971).**

$\log a(cm/s^2) = 2.80 + 0.20M - 1.10\log R$; Australia, Unconsolidated soil.

8. **Davenport, A.G. (1972).**

$a(cm/s^2) = 274e^{0.8M}R^{-1.64}$; Not applicable for $R \leq 15$ km

9. **Donovan, N.C. (1973).**

$a(cm/s^2) = 1080e^{0.5M}(R+25)^{-1.32}$; Rocky ground.

10. **Esteva, L. and R. Villaverde (1973).**

$a(cm/s^2) = 5600e^{0.8M}(R+40)^{-2}$; $\sigma_{\ln a} = 0.64$, $R \geq 15$ km

11. **Merz, H.A. and C.A. Cornell (1973).**

$a(cm/s^2) = 1200e^{0.8M}R^{-2}$; $\sigma_{\ln a} = 0.2$

12. **Orphal, D.L. and J.A. Lahoud (1974).**

$a(cm/s^2) = 64.75 \times 10^{0.4M}R^{-1.39}$; $\sigma_{\ln a} = 0.69$

California region, Rock and Alluvium, Not applicable for $R \leq 15$ km

13. **Bath, M. (1975).**

$a(cm/s^2) = 1.03h^{0.6}10^{0.54M}R^{-1.5}$; Tansania region, $R \geq 15$ km

APPENDIX–A Continued ...

14. Trifunac, M.D. (1976).

$$\log a(cm/s^2) = M + \log A_0(R) + 0.898p + 1.789M - 6.217 - 0.06s - 0.186M^2;$$

Applicable for M=4.8–7.5, $\log A_0(R)$ is Richter's attenuation function, p is confidence level, s=0 for alluvium, 2 for rock and 1 for intermediate type of geology.

15. McGuire R.K. (1977).

$$a(cm/s^2) = 472.0 \times 10^{0.278M}(R+25)^{-1.301}; \quad \sigma_{\ln a} = 0.62$$

Rock and Alluvium, Not applicable for $R \leq 15$ km

16. Ohashi et al (1977).

$$a(cm/s^2) = 46 \times 10^{0.208M}(R+10)^{-0.686}; \quad \text{Rock sites}$$

$$a(cm/s^2) = 24.5 \times 10^{0.333M}(R+10)^{-0.924}; \quad \text{Stiff soil}$$

Based on Japanese data.

17. Donovan, N.C. and A.E. Bornstein (1978).

$$a(g) = 2198e^{(0.046+0.193\ln R)M}R^{-2.1}(R+25)^{-2.515+0.211\ln R}$$

California region, Rock and stiff soil sites.

18. McGuire, R.K. (1978).

$$a(g) = 0.0306e^{0.89M}R^{-1.17}e^{-0.20s}; \quad \sigma_{\ln a} = 0.62$$

s = 0 for rock and 1 for soil sites in Western U.S.

19. Cornell, C.A., H. Banon and A. F. Shakal (1979).

$$a(g) = 0.863e^{0.86M}(R+25)^{-1.8}; \quad \sigma_{\ln a} = 0.57, \quad \text{Western U.S.}$$

20. Espinosa, A.F. (1980).

$$a(g) = 1.119 \times 10^{-6}e^{2.3M}R^{-0.11-0.22\ln R}; \quad \text{Western U.S.}$$

21. Battis, J. (1981).

$$a(g) = 0.3480e^{1.21M}(R+25)^{-2.08}; \quad \sigma_{\ln a} = 0.71, \quad \text{California region.}$$

$$a(g) = 0.0239e^{1.24M}(R+25)^{-1.24}; \quad \sigma_{\ln a} = 0.71, \quad \text{Central U.S.}$$

22. Campbell K.W. (1981)

$$a(g) = 0.0159e^{0.868M}\left(R + 0.0606e^{0.7M}\right)^{-1.09}; \quad \sigma_{\ln a} = 0.37,$$

Worldwide data, Rock sites, $R \leq 50$ km.

23. Hasegawa, H.S., P.W. Basham and M.J. Berry (1981).

$$a(g) = 1.02 \times 10^{-2}e^{1.3M}R^{-1.5}; \quad \text{Western Canada}$$

$$a(g) = 3.47 \times 10^{-3}e^{1.3M}R^{-1.1}; \quad \text{Eastern Canada}$$

24. Joyner, W.B. and D.M. Boore (1981).

$$a(g) = 0.0955e^{0.573M}\left(R^2+7.3^2\right)^{-0.5}e^{-0.00587\left(R^2+7.3^2\right)^{0.5}}; \quad \sigma_{\ln a} = 0.60,$$

Western North America.

APPENDIX–A Continued ...

25. Nuttli, O.W. and R.B. Herrmann (1984).

$a(g) = 3.79 \times 10^{-3} e^{1.15M}(R^2 + 0.000346e^{2.1M})^{-0.415} e^{-0.00159R}$; $\sigma_{\ln a} = 0.55$

Mississippi Valley

26. Sabetta , F. and A. Pugliese (1987).

$\log a(g) = -1.562 + 0.306M - \log(R^2 + 5.8^2)^{\frac{1}{2}} + 0.169s$;

s=0 for rock sites and 1 for soft sites, Italian data.

27. Peng, K.Z., F.T. Wu and L. Song (1985).

$\log a(cm/s^2) = -0.474 + 0.613M - 0.873 \log R - 0.00206R$; NE China

$\log a(cm/s^2) = 0.437 + 0.454M - 0.739 \log R - 0.00279R$; NW China

28. Abrahamson, N.A. and J.J. Litehiser (1989).

$\log a(g) = -0.62 + 0.177M - 0.982 \log(R + e^{0.284M}) + 0.132F - 0.0008E_r$; $\sigma_{\ln a} = 0.277$

Worldwide data, F = 1 for reverse or reverse oblique events, 0 otherwise.

$E_r = 1$ for interplate events and 0 for intraplate events.

29. Fukushima, Y and T. Tanara (1990).

$\log a(cm/s^2) = 0.41M - \log(R + 0.032 \times 10^{0.41M}) - 0.0034R + 1.30$; Japan

30. Gupta I.D., V. Rambabu and R.G. Joshi (1991).

$\log a(cm/s^2) = 2.64 - 0.01197R - 0.09952 \log R - 0.6476M + 0.10634M^2$

Koyna region, India.

31. Crouse, C.B. (1991).

$\ln a(cm/s^2) = 6.36 + 1.76M - 2.731 \ln(R + 1.58e^{0.608M}) + 0.00916h$; $\sigma_{\ln a} = .773$

Cascadia subduction zone.

32. Ambraseys, N.M. and J.J. Bommer (1991).

$\log a(g) = -0.87 + 0.217M - \log R - 0.00117R$; $\sigma_{\log a} = 0.26$,

Europe

33. Theodulidin, N.P. and B.C. Papazachos (1992).

$\ln a(cm/s^2) = 3.88 + 1.12M - 1.65 \ln(R + 15) + 0.41s$; $\sigma_{\ln a} = 0.71$

s = 1 for rock and 0 for alluvial sites, Greece.

34. Niazi, M. and Y. Bozorgnia (1991).

$\ln a(g) = -5.503 + 0.936M - 0.816 \ln(R_h + 0.407e^{0.455M})$; $\sigma_{\ln a} = 0.461$,

NE Taiwan.

35 Tento, A., L. Franceschina and A. Marcellini (1992).

$\ln a(cm/s^2) = 4.73 + 0.52M - \ln R - 0.002R$; $\sigma_{\ln a} = 0.67$, Italian sites.

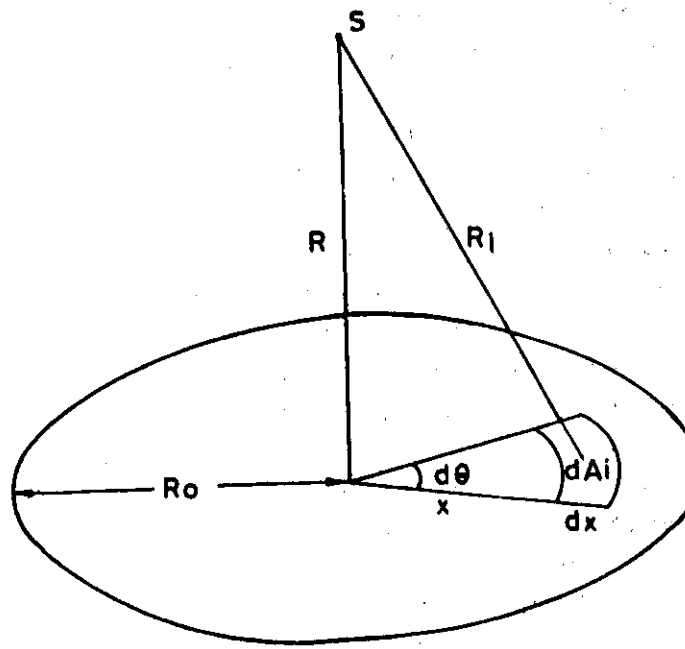

Fig.B.1 A circular fault-plane of radius R_o with the site of observation, S, located on its axis at distance R from the centre. The total source area, A, of the fault is assumed to consist of a large number of elementary subsources, with the ith element of area, dA_i, located at a distance R_i from the site S.

APPENDIX–B

EQUIVALENT SOURCE–TO–SITE DISTANCE

If the entire seismic energy due to an earthquake is assumed to originate from a single point, the total power of the radiated seismic energy received at a site at distance R from the source can be written at frequency ω as (Gupta et al., 1994)

$$E(\omega) = C^2\omega^4 M_o^2(\omega)\frac{e^{-\omega R/\beta Q}}{R^2} \qquad (B.1)$$

In this expression, C is a constant defined in terms of the radiation pattern of seismic waves and density, ρ, and shear-wave velocity, β, of the medium. The function $M_o(\omega)$ is known as seismic moment density. The exponential term defines the anelastic attenuation of the waves with Q as the quality constant. For high–frequency ground motion at close distances, the anelastic attenuation effects would be negligible, and hence eqn. (B.1) can be approximated by

$$E(\omega) = C^2\omega^4\frac{M_o^2(\omega)}{R^2} \qquad (B.2)$$

The point–source approximation is not valid for an earthquake, which, in fact, is characterized by rupturing of a large fault area. To consider the effect of the finite size of the seismic source for sites at close distances, let the fault be idealized by a circular area of radius R_o and the site of observation, S, be located at a distance R on the axis of the circle as shown in Fig. B.1. Now consider the total area A of the fault to be consisted of a large number of small elements, each one of which acts as an independent seismic subsource. Assuming that the total source density, $M_o^2(\omega)$, is distributed uniformly over the entire source area, A, the energy radiated from an element of area dA_i at distance R_i can be written as

$$E_i(\omega) = C^2\omega^4\frac{M_o^2(\omega)}{R_i^2}\frac{dA_i}{A}; \quad A = \pi R_o^2 \quad and \quad R_i = \left(x^2 + R^2\right)^{1/2} \qquad (B.3)$$

Further, assuming that the rupture of various elementary areas occur randomly with uniform probability, the energy spectrum of the total ground motion at site S can also be expressed as (Lee, 1964)

$$E(\omega) = \sum_i E_i(\omega) = C^2\omega^4 M_o^2(\omega)\frac{1}{\pi R_o^2}\sum_i \frac{dA_i}{R_i^2} \qquad (B.4)$$

Comparing this expression with that of eqn. (B.2) indicates that the effect of the fault size on the high–frequency ground motion in the near–field can be reproduced by a virtual point source at an equivalent distance R_{eq}, such that

$$R_{eq}^{-2} = \frac{1}{\pi R_o^2}\sum_i \frac{dA_i}{R_i^2} \qquad (B.5)$$

Assuming that the number of source elements are so large that the summation in eqn. (B.5) can be replaced by integration, eqn. (B.5) gives

$$R_{eq}^{-2} = \frac{1}{\pi R_o^2} \int_0^{R_o} \int_0^{2\pi} \frac{x dx d\theta}{x^2 + R^2} = \frac{1}{R_o^2} \ln \left(\frac{R^2 + R_o^2}{R^2} \right) \tag{B.6}$$

From this, the equivalent distance, R_{eq}, is given as

$$R_{eq} = R_o \left[\ln \left(\frac{R^2 + R_o^2}{R^2} \right) \right]^{-1/2} \tag{B.7}$$